

# ANALYSIS OF FRACTURE BEHAVIOUR IN ESP GLASSES

Vincenzo M. Sglavo and Christian Lorenzini

DIMTI, University of Trento, Via Mesiano 77, 38050 Trento (ITALY)

## ABSTRACT

ESP (Engineered Stress Profile) glasses are innovative materials characterized by peculiar mechanical properties such as high failure resistance and limited strength scatter. These properties arise from the engineered residual stress frozen within the material that promotes the stable growth of surface defects before final failure. Other interesting features of ESP glasses are the insensitivity to fatigue and the fine fragmentation upon failure, this latter preventing the visual analysis of fracture events. The fracture behaviour of ESP glass is analytically studied in the present work with the aim to point out possible correlations between residual stresses, crack propagation and final strength. Initially a simple single-crack model usually considered for the design of ESP glasses is reviewed and associated limitations are discussed. Then, multiple cracking phenomenon occurring before final failure is investigated. The analysis is carried out referring to two different ESP glasses produced and characterized in previous works.

## 1 INTRODUCTION

ESP (Engineered Stress Profile) glasses represent an innovative class of materials characterized by high mechanical resistance and limited strength scatter (Green *et al.* [1], Sglavo *et al.* [2]). The name arises from the “engineering” of the stress profile frozen within the material usually characterized by a maximum compression at a certain depth from the surface and by a quite high negative gradient on the surface. Typical residual stresses generated in two different silicate glasses by a double ion-exchange process are shown in Fig. 1 (Sglavo *et al.* [2]). The peculiar residual stress profile accounts for the high mechanical resistance and for the stable propagation and arrest of surface defects before final failure, these resulting in an insensitiveness of the strength from surface flaw sizes.

ESP glasses show other interesting features such as multiple surface cracking, fine fragmentation upon failure and limited fatigue sensitivity. The fine fragmentation prevents the direct observation of fracture behaviour and limits the analysis of crack arrest and stable growth phenomena, which may influence the mechanical performance of the material. In this work, the fracture behaviour of ESP glass is studied by analytical methods with the aim to point out possible correlations between the residual stress profile, crack propagation and final strength. Evaluations are performed referring to the two glasses reported in Fig. 1, corresponding to two glasses previously studied (Sglavo *et al.* [2]). Initially the simple crack model usually considered for the design and analysis of ESP glasses is reviewed and associated limitations are discussed. Then, multiple cracking phenomenon occurring before final failures is investigated.

## 2 FRACTURE BEHAVIOUR ANALYSIS

In order to analyze the effect of residual stresses on crack propagation and failure resistance, the simple model depicted in Fig. 2 can be considered. The residual stress, which is a function of the distance from the surface only, is associated to a stress intensity factor defined as (Lawn [3]):

$$K_{res} = \frac{\psi}{\sqrt{\pi a}} \int_0^a g(x) \sigma_{res}(x) dx \cdot \quad (1)$$

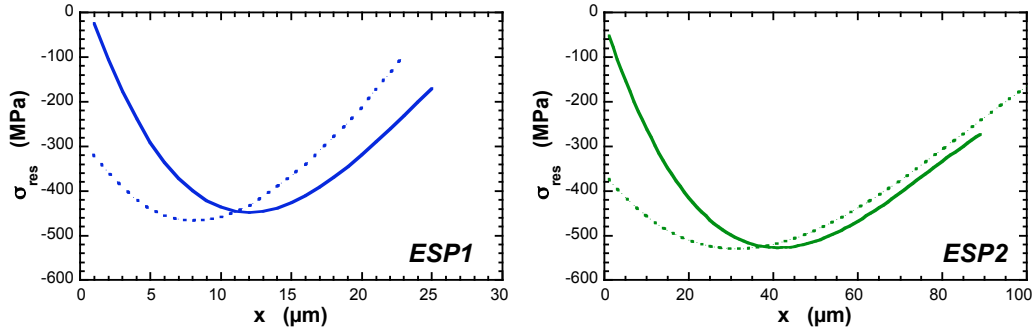


Figure 1: Residual stress profile for two ESP silicate glasses. Dashed curves represent the stress profile after the first ion-exchange.

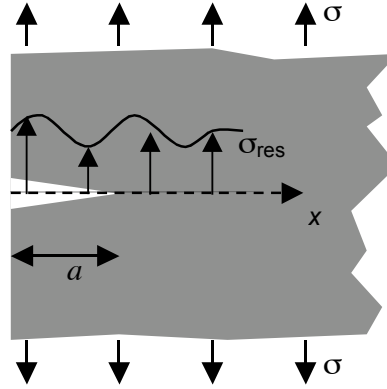


Figure 2: Crack system used for the design of ESP glasses.

being  $\psi = 1.12$  is a shape factor and  $g(x) = 2a/\sqrt{a^2 - x^2}$  the so called Green's function (Lawn [3]).

The generic system in Fig. 2 can be also subjected to external loads; when external tensile stresses are considered (as in Fig. 2), the associated stress intensity factor is (Lawn [3]):

$$K_{appl} = \psi \sigma \sqrt{\pi a} \quad (2)$$

Crack propagation occurs when the sum ( $K_{res} + K_{appl}$ ) equals the fracture toughness,  $K_C$ , of the material. If the residual stresses are virtually considered as a material characteristic, the apparent fracture toughness can be defined by combining  $K_C$  with the stress intensity factor associated to  $\sigma_{res}$ :

$$K_C^* = K_C - K_{res}. \quad (3)$$

It is clear that compressive (negative) residual stresses have beneficial effects on the material resistance, as the associated apparent fracture toughness becomes an increasing function of crack size. This effect is particularly efficient in ESP glass. By considering the residual stress profile shown in Fig. 1, a well-developed  $R$ -curve can be calculated as reported in Fig. 3. One can easily observe that the specific shape of  $K_C^*$  promotes the stable growth of surface defects in a well-

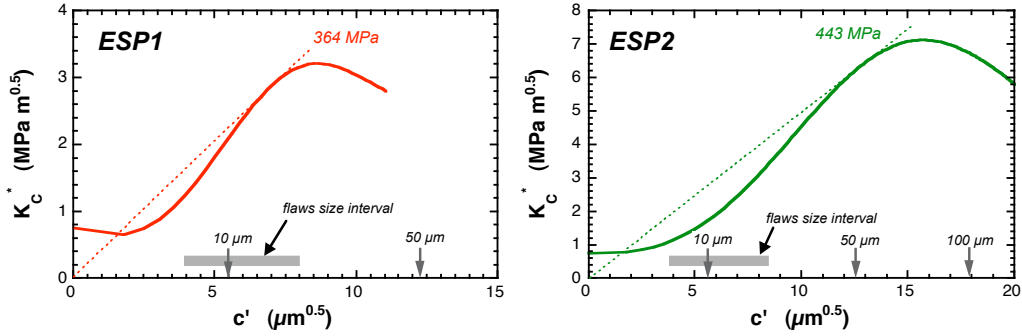


Figure 3: Apparent fracture toughness curves. The dashed lines represent the graphical construction used for the calculation of the reported final strength ( $c' = (\pi c)^{0.5}$ ).

defined interval. If the initial surface flaws fall in such interval, an unique-value strength can be obtained from the graphical construction reported in Fig. 3. Most of the original surface defects actually sit in the specified interval, thus allowing the calculation of a theoretical strength value, as reported in Fig. 3. Strength values measured for the two considered glasses are equal to  $426 \pm 18$  MPa (glass ESP1) and  $553 \pm 45$  MPa (glass ESP2) and are therefore substantially higher than the theoretical one (Sglavo *et al.* [2]). This discrepancy can be accounted for the oversimplified model used for the mechanical analysis.

As reminded before, multiple cracks propagate in a stable manner on the tensile surface of ESP glass before final failure forming an array of through-thickness cracks (Sglavo and Green [4], Green *et al.* [5]). It is clear that such phenomenon can influence the compliance of the material and, therefore, the final resistance. A more detailed crack model can be therefore considered as shown in Fig. 4. In this case the stress intensity factor associated to the external load depends on the crack depth,  $a$ , and spacing,  $d$ , through the following equation (Murakami [6]):

$$K_{app} = F\left(\frac{a}{d}\right)\sigma\sqrt{\pi a} \quad (4)$$

where  $F$  is a decreasing function of  $a/d$  (Murakami [6]). An interesting observation is that for  $a/d > 1$ ,  $F \approx (d/a)^{0.5}$  and  $K_{app} \approx \sigma (d/2)^{0.5}$ ; therefore, when several surface cracks are generated on the sample, the applied stress intensity factor becomes independent on crack depth.

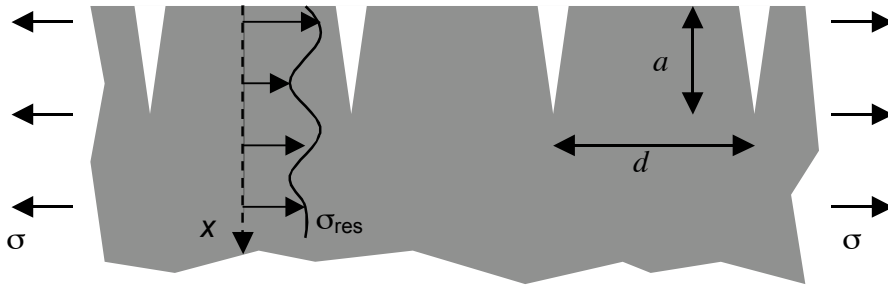


Figure 4: Crack system used for the analysis of multicracking phenomenon.

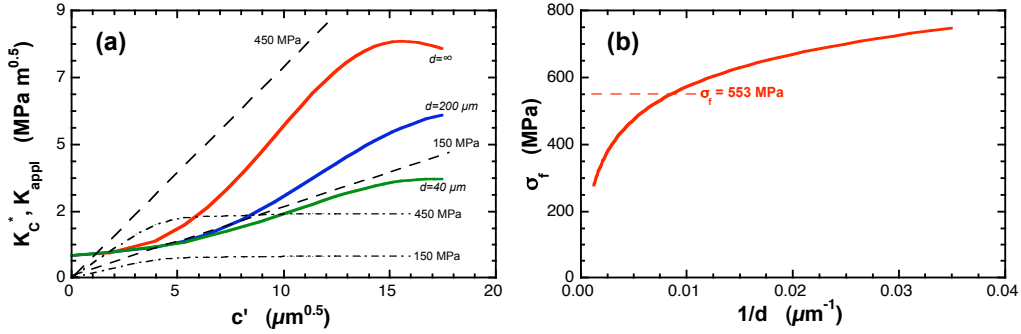


Figure 5: (a)  $K_C^*$  (continuous lines) and  $K_{appl}$  (dashed lines) calculated on the basis of the model shown in Fig. 4 for glass ESP1. Dashed and dash and points curves correspond to  $d = \infty$  and  $d = 40 \mu\text{m}$ , respectively (the applied stress is reported). (b) Theoretical strength as a function of  $1/d$  calculated from diagrams similar to (a) (the measured strength is shown).

Also the stress intensity factor associated to residual stresses assumes a different notation (Fett and Munz [7]):

$$K_{res} = \sqrt{\frac{2}{\pi a} \int_0^a G(x/a) \sigma_{res}(x) dx} \quad (5)$$

where  $G(x/a)$  is given in (Fett and Munz [7]). The apparent fracture toughness changes accordingly. The assumption is made here that the residual stress profile does not change as crack propagation occurs. As shown in Fig. 5(a), for an increasing number of surface cracks (*i.e.* decreasing  $d$ ), both  $K_C^*$  and  $K_{appl}$  decrease. By using a graphical construction similar to that shown in Fig. 3 the theoretical strength can be calculated as a function of  $d$ . An example is reported in Fig. 5(b) and one can realize that the surface multicracking accounts for a shielding effect that results in higher and higher strength values provided the crack spacing decreases. Therefore the proposed model, based on mechanical assumptions only, does not furnish information on the finite final strength value really measured.

Further information regarding the evolution of crack spacing upon loading, an energetic approach, similar to the Griffith's thermodynamic concept, can be considered. The total energy,  $U$ , of the system shown in Fig. 4 is a function of the parameters  $a$ ,  $d$  and  $\sigma$ . If any kinetic contribution is neglected, the energy variation can be expressed as (Lawn [3]):

$$\Delta U = \Gamma - W \quad (6a)$$

where

$$\Gamma = 2\gamma a/d, \quad \gamma = \frac{K_C^2}{2E} \quad W = \frac{1}{d} \int_0^a \frac{K_I^2}{E} dx \quad \text{and} \quad K_t = K_{appl} + K_C^* \quad (6b)$$

$E$  being the elastic modulus. The stationary points of the energy function can be evaluated by solving the following system:

$$\begin{cases} \frac{\partial \Delta U}{\partial a} = 0 \\ \frac{\partial \Delta U}{\partial d} = 0 \end{cases} \quad \Delta U \leq 0 \quad (7)$$

A typical set of results is reported in Fig. 6. In this case the effect of the environment is also taken into account. On the basis of previous results (Sglavo and Green [8]), the sub-critical growth is simulated by using a lower fracture toughness value ( $0.5 \text{ MPa m}^{0.5}$  instead of  $0.75 \text{ MPa m}^{0.5}$  in

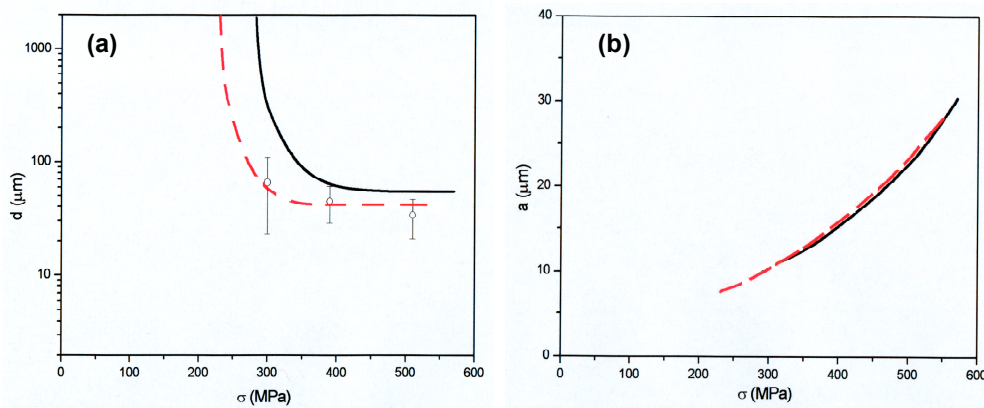


Figure 6: Evolution of crack spacing (a) and depth (b) as function of the applied load. Dashed curves correspond to the behaviour in water. Experimental crack spacing data are shown.

Eq. (6). Both in inert and aggressive environment crack spacing (Fig. 6(a)) suddenly decreases, upon loading, above a certain critical applied stress, reaching a constant value. Measurements of crack spacing in samples tested in humid environment well agree with the results obtained through the proposed energetic approach. On the other hand, crack depth (Fig. 6(b)) results to be an increasing function of the applied load. The multicracking phenomenon can be therefore regarded as a two-step process: above a certain critical load surface flaws grow into an array of through-thickness cracks whose final spacing ( $d^*$ ) depends on the material and the environment. Then if the load is increased further, the crack depth can increase accordingly. As shown in Fig. 6(a) the proposed model well simulates the crack spacing evolution as it was measured on samples tested in humid environment (Sglavo and Green [9]).

At this point, on the basis of previous arguments, once the crack spacing is defined, one can predict the mechanical resistance. Also in this case the theoretical values exceed the measured ones. Values equal to 570 MPa and 750 MPa can be evaluated for the two ESP glasses considered in this work. Several effects can be accounted to explain the observed discrepancies. First of all crack spacing is not constant and through-thickness crack propagation does not occur simultaneously. Therefore, once two crack propagate at distance lower than  $2d^*$ , it is unlikely that a crack is formed between them, the crack spacing remaining larger than  $2d^*$ . In addition, failure can occur from defects other than the through-thickness cracks that become critical at lower loads. Then the residual stress can relax when crack propagation occurs thus diminishing the strengthening effect. Finally, some of the through-thickness cracks experience some deflection above a certain load level especially in C glass (Sglavo and Green [9]), and this complicates the mechanical model shown in Fig. 4 further.

#### 4 REFERENCES

- [1] D. J. Green, R. Tandon and V. M. Sglavo, Crack Arrest and Multiple Cracking in Glass Using Designed Residual Stress Profiles, *Science*, 283 (1999) 1295-97
- [2] V.M Sglavo, A. Prezzi and T. Zandonella, ESP (Engineered Stress Profile) silicate glass, High strength material, insensitive to surface defects and fatigue, *Adv. Eng. Materials*, 6[5], 344-

349, 2004.

- [3] B. R. Lawn, Fracture of brittle solids, 2<sup>nd</sup> Ed., Cambridge University Press: Cambridge, UK (1993).
- [4] V. M. Sglavo and D. J. Green, Flaw Insensitive Ion-Exchanged Glass: II, Production and Mechanical Performance, J. Am. Ceram. Soc., 84 [8] (2001) 1832-38.
- [5] D.J. Green, V.M. Sglavo, E.K. Beauchamp and S.J. Glass, Designing residual stress profiles to produce flaw-tolerant glass, Fracture Mechanics of Ceramics, Vol. 13, Ed. R.C. Bradt et al., Kluwer Academic / Plenum Press, 2002, pp.99-105.
- [6] Y. Murakami, Stress Intensity Factors Handbook, Vol. 2, pp. 114-117, Pergamon Press, 1970.
- [7] T. Fett and D. Munz, Stress Intensity Factors and Weight Functions, Computational Mechanics Publications, Southampton, UK and Boston, 1998.
- [8] V. M. Sglavo and D. J. Green, Indentation Determination of Fatigue Limits in Silicate Glasses, J. Am. Ceram. Soc., 82 [5] (1999) 1269-74.
- [9] V. M. Sglavo and D. J. Green, In-situ Fractography of ESP Glasses, manuscript in preparation.